C. R. Mecanique 344 (2016) 151–166

Contents lists available at ScienceDirect

Comptes Rendus Mecanique

www.sciencedirect.com

# Nonlinear vibrations of buckled plates by an asymptotic numerical method

Lahcen Benchouaf *, El Hassan Boutyour

*Department of Applied Physics, Faculty of Sciences and Technology, Hassan 1st University, PO Box 577, Settat, Morocco*

A R T I C L E I N F O

*Article history:*
Received 27 October 2015
Accepted 5 January 2016
Available online 3 February 2016

*Keywords:*
Nonlinear vibrations
Buckling
Von Karman plate
Asymptotic numerical method
Harmonic balance method
Finite-element method

A B S T R A C T

This work deals with nonlinear vibrations of a buckled von Karman plate by an asymptotic numerical method and harmonic balance approach. The coupled nonlinear static and dynamic problems are transformed into a sequence of linear ones solved by a finite-element method. The static behavior of the plate is first computed. The fundamental frequency of nonlinear vibrations of the plate, about any equilibrium state, is obtained. To improve the validity range of the power series, Padé approximants are incorporated. A continuation technique is used to get the whole solution. To show the effectiveness of the proposed methodology, numerical tests are presented.



## 1. Introduction

Vibrations and buckling are common instability phenomena accompanied, generally, by large displacements and important changes in the shape of structures widely used in various industrial fields such as civil engineering, mechanics, aerospace, etc. For appropriate design, it is necessary to develop analytical, numerical or experimental tools able to analyze these problems in order to predict accurately critical loads and natural frequencies (instability and resonance regions). In the literature, various approaches coupling the two problems were developed. A relatively simple one consists, first, in computing static equilibrium branches with the corresponding critical loads and, secondly, in analyzing the vibrations of the structure about a given equilibrium position of the pre- or post-buckled domain. The majority of the realized works, using the indicated approach, concern only linear theory and consider beams, plates or shells structures. These studies show, especially, that the first frequencies can define bifurcation indicators that can be employed advantageously in the non-destructive control. Furthermore, some papers consider non-conservative loads leading to complex instabilities called flutter phenomena. But it is known that, when a shell is deflected more than approximately one-half of its thickness, significant geometrical nonlinearities are induced and a variation of the frequency resonance with the vibration amplitude is shown [1]. However, to the author's knowledge, only a few works have shown an interest in the coupling of the buckling and vibrations and taken into account these nonlinearities [2–12]. Min and Eisley [2] and Tseng and Dugundji [3] adopted analytical procedures based on Galerkin method and modal approximation to study beams subjected to in-plane load. Note that, experimental results were presented in the last paper. Using the same procedures with elliptic integrals, Lesatri and Hanagul [4] studied beams with elastic end restraints. Employing Kirchhoff plate theory and Harmonic balance method, Mahdavi et al. [5] examined the effect of in-plane load on embedded single layer graphene sheet (SLGS) in a polymer

* Corresponding author.
*E-mail address:* l.benchouaf@uhp.ac.ma (L. Benchouaf).

http://dx.doi.org/10.1016/j.crme.2016.01.002
1631-0721/

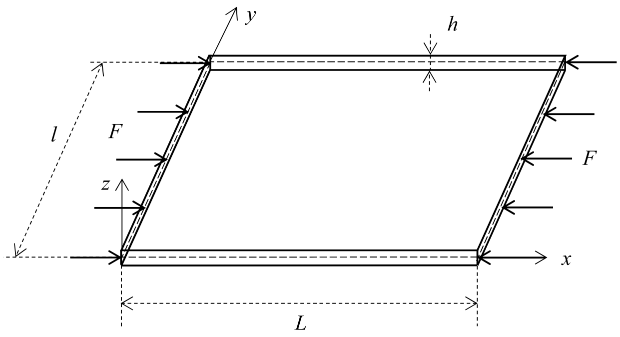


**Fig. 1.** Geometry and coordinate system of a rectangular plate.

matrix aroused by nonlinear Van Der Waals forces. Shojaei et al. [6] proposed a numerical approach based on Galerkin procedure and a discretization of the space and time domains to investigate Euler–Bernoulli beams with different boundary conditions. Ansari et al. [7] studied microscale Euler–Bernoulli beams employing a couple stress theory. They also considered post-buckled von Karman nanoplates [8]. Based on a high order shear deformation theory, on a Galerkin method and a Newton–Raphson iterative procedure, Girish and Ramachandra [9] investigated laminated composite plates, with initial geometric imperfections and subjected to a uniform temperature distribution through the thickness. Li et al. [10] used von Karman plate theory, Kantorovich time-averaging method and a shooting method to study circular orthotropic plates with a centric rigid mass. Xia and Shen [11,12] considered sandwich plates with functionally graded material FGM face sheets and FGM plates with a layer of piezoelectric actuators in thermal environments and subjected to a compression load. The used formulation is based on a high-order shear deformation theory and takes into account thermo-piezoelectric effects. The motion equations are solved by a perturbation technique.

The aim of the present work consists in studying the nonlinear free vibrations of von Karman plates about a static equilibrium of the pre- or post-buckled domain, by an asymptotic numerical method (ANM) combined to a harmonic balance method. The unknowns of the problem (solution branches, natural frequencies and mode shapes) are determined by a perturbation technique whose terms are computed by a finite-element method. The coupled nonlinear problems (static and dynamic) are transformed into a sequence of linear ones with only two operators to be inverted. In this approach, one searches, first, the equilibrium branches and the bifurcation points. Secondly, the backbone curves, related to the fundamental frequency of nonlinear free vibration of the structure about any equilibrium position of pre and post buckling domain, are determined. At each stage of the proposed algorithm, Padé approximants are incorporated to improve the validity range of the power series and to reduce the computational cost. The whole solution branches at large displacements are derived by the continuation procedure. To show the effectiveness and the reliability of the proposed methodology, numerical tests are presented.

## 2. Formulation of the problem

The main objective of this paper consists in developing a methodological approach based on the asymptotic numerical method and coupling buckling and nonlinear free vibration of thin plates subjected to uniaxial load. Here, one follows exactly the same methodology as that adopted in [13]. After determining the static fundamental branch, the bifurcation point and the bifurcated branches, the backbone curve corresponding to the fundamental frequency of the nonlinear vibrations of the plate about any equilibrium state of the pre- or post-buckled domain is determined.

### 2.1. Governing equation of static equilibrium

Let us consider an elastic and homogeneous rectangular plate of thickness $h$, length $L$, width $l$, middle surface $\Omega$, density mass $\rho$, Young modulus $E$, Poisson's ratio $\nu$. In a rectangular coordinate reference frame $(O; x, y, z)$, the displacement components of a middle surface point of coordinates $(x, y, z)$ are denoted by $u$, $v$, and $w$ in the $x$, $y$ and $z$ directions, respectively. One assumes that the plate is subjected to a uniform axially compressive force $F$ per unit length, in the $x$-direction, along the edges $x = 0, L$ (see Fig. 1).

The governing equation of the nonlinear static behavior can be derived by the von Karman theory. To use easily a perturbation technique, a mixed principal is required. The stationarity of the Hellinger–Reissner functional gets [14]:

$$\overline{\mathrm{L}}\big(\mathrm{U^s}\big) + \overline{\mathrm{Q}}\big(\mathrm{U^s}, \mathrm{U^s}\big) - \lambda F = 0 \tag{1}$$

where $\mathrm{U^s} = \{\mathrm{u^s}, \mathrm{v^s}, \mathrm{w^s}, \mathrm{N^s}\}^{\mathrm{t}}$ is a mixed unknown vector, the linear operator $\overline{\mathrm{L}}(\cdot)$ and the quadratic one $\overline{\mathrm{Q}}(\cdot,\cdot)$ are defined by:

$$\big\langle \overline{\mathrm{L}}\big(\mathrm{U^s}\big), \delta\overline{\mathrm{U}}\big\rangle = \int_{\Omega} \big\{\delta\mathrm{N} : \big(\Gamma^{\mathrm{l}}\big(\mathrm{u^s}\big) - [\mathrm{C_m}]^{-1} : \mathrm{N^s}\big) + \delta\Gamma^{\mathrm{l}}(\delta\overline{\mathrm{u}}) : \mathrm{N^s} + \delta\kappa : [\mathrm{C_b}] : \kappa^{\mathrm{s}}\big\} \mathrm{d}\Omega \tag{2}$$

$$\langle \overline{\mathrm{Q}}(\mathrm{U^s}, \mathrm{U^s}), \delta\overline{\mathrm{U}}\rangle = \int_{\Omega} \{\delta \mathrm{N} : \Gamma^{\mathrm{nl}}(\mathrm{u^s}, \mathrm{u^s}) + \mathrm{N^s} : 2\Gamma^{\mathrm{nl}}(\mathrm{u^s}, \delta\overline{\mathrm{u}})\} \mathrm{d}\Omega \tag{3}$$

The last term of Eq. (1) is given by:

$$\langle F, \delta\overline{\mathrm{U}}\rangle = \int_{\Omega} \{f_u \delta\overline{\mathrm{u}} + f_v \delta\overline{\mathrm{v}}\} \mathrm{d}\Omega \tag{4}$$

where $\Gamma = \Gamma^{\mathrm{l}}(\mathrm{u^s}) + \Gamma^{\mathrm{nl}}(\mathrm{u^s}, \mathrm{u^s})$ is the Green–Lagrange strain decomposed into a linear and a quadratic part, $\kappa^s$ is the bending strain, $\mathrm{N^s}$ is the membrane force per unit length, $[\mathrm{C_m}]$ and $[\mathrm{C_b}]$ are the stiffness matrices of membrane and bending, respectively. $\lambda$ is a scalar load parameter, $f_u$ and $f_v$ are the components of the applied force $F$ in the $x$ and $y$ direction, respectively.

### *2.2. Vibration about a static equilibrium configuration*

One assumes that, for a given applied load, the plate oscillates about its corresponding equilibrium deformed state $\mathrm{U^s}$. These oscillations are described by the time-dependent mixed vector $\overline{\mathrm{U}}(\overline{\mathrm{u}}, \overline{\mathrm{v}}, \overline{\mathrm{w}}, \mathrm{t})$. The global response is assumed to be the sum of the static part and dynamic one [13]:

$$\mathrm{U^s}(\mathrm{u^s}, \mathrm{v^s}, \mathrm{w^s}) + \overline{\mathrm{U}}(\overline{\mathrm{u}}, \overline{\mathrm{v}}, \overline{\mathrm{w}}, \mathrm{t}) \tag{5}$$

Note that the static deformed configuration can correspond to a pre- or post-buckled state. Based on Hamilton's principle and neglecting in-plane and rotary inertia terms, the oscillations of the plate about the static deformed state are described by the following equation:

$$\overline{\mathrm{L}}(\mathrm{U^s} + \overline{\mathrm{U}}) + \overline{\mathrm{Q}}(\mathrm{U^s} + \overline{\mathrm{U}}, \mathrm{U^s} + \overline{\mathrm{U}}) + \overline{\mathrm{M}}(\ddot{\overline{\mathrm{U}}}) - \lambda F = 0 \tag{6}$$

where the inertia operator is given by:

$$\langle \overline{\mathrm{M}}(\ddot{\overline{\mathrm{U}}}), \delta\overline{\mathrm{U}}\rangle = \rho \mathrm{h} \int_{\Omega} \{\ddot{\overline{\mathrm{u}}}\delta\overline{\mathrm{u}} + \ddot{\overline{\mathrm{v}}}\delta\overline{\mathrm{v}} + \ddot{\overline{\mathrm{w}}}\delta\overline{\mathrm{w}}\} \mathrm{d}\Omega \tag{7}$$

Let us recall that the nonlinear free vibrations of the unloaded plate can be investigated by numerically solving Eq. (6) with $\mathrm{U^s} = 0$. On the other hand, putting $\overline{\mathrm{U}} = 0$ into Eq. (6), leads to the nonlinear static analysis of the plate. The governing equation of the nonlinear free vibrations of the plate about a static equilibrium state is deduced from Eq. (6) taking into account Eq. (1):

$$\overline{\mathrm{L}}(\overline{\mathrm{U}}) + 2\overline{\mathrm{Q}}(\mathrm{U^s}, \overline{\mathrm{U}}) + \overline{\mathrm{Q}}(\overline{\mathrm{U}}, \overline{\mathrm{U}}) + \overline{\mathrm{M}}(\ddot{\overline{\mathrm{U}}}) = 0 \tag{8}$$

Of course, neglecting $\overline{\mathrm{Q}}(\overline{\mathrm{U}}, \overline{\mathrm{U}})$ in Eq. (8) leads to linear vibrations problem of buckled plate which was largely discussed in [13] for various shell structures. Here, this term is taken into account. To solve the problem, one adopts the harmonic balance method [15–17]. The components of the dynamic part of the global displacement vector are assumed to be in the following form:

$$\begin{aligned}
\overline{\mathrm{u}}(\mathrm{x}, \mathrm{y}, \mathrm{t}) &= \mathrm{u}(x, y) \cos^2(\omega t) \\
\overline{\mathrm{v}}(\mathrm{x}, \mathrm{y}, \mathrm{t}) &= \mathrm{v}(x, y) \cos^2(\omega t) \\
\overline{\mathrm{w}}(\mathrm{x}, \mathrm{y}, \mathrm{t}) &= \mathrm{w}(x, y) \cos(\omega t)
\end{aligned} \tag{9}$$

where $\omega$ denotes the natural frequency.

To study the history of the solution corresponding to a period, the initial time is set as $t_0 = 0$ and the final time $t_1 = 2\pi/\omega$. Using the expressions given by Eq. (9) and after integration of Eq. (8) over the time range, one gets:

$$\begin{aligned}
&\int_{\Omega} \left\{-\delta \mathrm{N}^1 : [\mathrm{C_m}]^{-1} : \mathrm{N}^1 + \frac{3}{4}\delta \mathrm{N}^2 : (\gamma^{\mathrm{l}}(\mathrm{u}) - [\mathrm{C_m}]^{-1} : \mathrm{N}^2) + \frac{3}{4}\gamma^{\mathrm{l}}(\delta \mathrm{u}) : \mathrm{N}^2 + \delta\kappa : [\mathrm{C_b}] : \kappa\right\} \mathrm{d}\Omega \\
&\quad + \int_{\Omega} \{\delta \mathrm{N}^1 : 2\gamma^{\mathrm{nl}}(\mathrm{u^s}, \mathrm{u}) + \mathrm{N}^1 : 2\gamma^{\mathrm{nl}}(\mathrm{u^s}, \delta \mathrm{u}) + \mathrm{N^s} : 2\gamma^{\mathrm{nl}}(\mathrm{u}, \delta \mathrm{u})\} \mathrm{d}\Omega \\
&\quad + \frac{3}{4}\int_{\Omega} \{\delta \mathrm{N}^2 : \gamma^{\mathrm{nl}}(\mathrm{u}, \mathrm{u}) + \mathrm{N}^2 : 2\gamma^{\mathrm{nl}}(\mathrm{u}, \delta \mathrm{u}) +\} \mathrm{d}\Omega - \omega^2 \rho \mathrm{h} \int_{\Omega} \{\mathrm{u}\delta \mathrm{u} + \mathrm{v}\delta \mathrm{v} + \mathrm{w}\delta \mathrm{w}\} \mathrm{d}\Omega = 0; \\
&\forall(\delta \mathrm{u}, \delta \mathrm{v}, \delta \mathrm{w}, \delta \mathrm{N}^1, \delta \mathrm{N}^2)
\end{aligned} \tag{10}$$

where $\mathrm{N}^1 = [\mathrm{C_m}] : \{\gamma^{\mathrm{nl}}(\mathrm{u^s}, \mathrm{u})\}$ and $\mathrm{N}^2 = [\mathrm{C_m}] : \{\gamma^{\mathrm{l}}(\mathrm{u}) + \gamma^{\mathrm{nl}}(\mathrm{u}, \mathrm{u})\}$.

It is clearly seen that the dependence in time is transformed into a frequency one. The last variational problem can be written in an operational form:

$$\mathrm{L}(\mathrm{U}) + 2\mathrm{Q}\big(\mathrm{U}^{\mathrm{s}}, \mathrm{U}\big) + \mathrm{Q}(\mathrm{U}, \mathrm{U}) - \omega^2 \mathrm{M}(\mathrm{U}) = 0 \tag{11}$$

where $\mathrm{U} = (u, v, w, \mathrm{N}^1, \mathrm{N}^2)$ is a mixed unknown vector and

$$\big\langle \mathrm{L}(\mathrm{U}), \delta\mathrm{U}\big\rangle = \int_\Omega \left\{ -\delta\mathrm{N}^1 : [\mathrm{C_m}]^{-1} : \mathrm{N}^1 + \frac{3}{4}\delta\mathrm{N}^2 : \big(\gamma^{\mathrm{l}}(\mathrm{u}) - [\mathrm{C_m}]^{-1} : \mathrm{N}^2\big) + \frac{3}{4}\gamma^{\mathrm{l}}(\delta\mathrm{u}) : \mathrm{N}^2 + \delta\kappa : [\mathrm{C_b}] : \kappa \right\} \mathrm{d}\Omega \tag{12a}$$

$$2\big\langle \mathrm{Q}\big(\mathrm{U}^{\mathrm{s}}, \mathrm{U}\big), \delta\mathrm{U}\big\rangle = \int_\Omega \big\{\delta\mathrm{N}^1 : \gamma^{\mathrm{nl}}\big(\mathrm{u}^{\mathrm{s}}, \mathrm{u}\big) + \mathrm{N}^1 : \gamma^{\mathrm{nl}}\big(\mathrm{u}^{\mathrm{s}}, \delta\mathrm{u}\big) + \mathrm{N}^{\mathrm{s}} : \gamma^{\mathrm{nl}}(\mathrm{u}, \delta\mathrm{u})\big\} \mathrm{d}\Omega \tag{12b}$$

$$\big\langle \mathrm{Q}(\mathrm{U}, \mathrm{U}), \delta\mathrm{U}\big\rangle = \frac{3}{4}\int_\Omega \big\{\delta\mathrm{N}^2 : \gamma^{\mathrm{nl}}(\mathrm{u}, \mathrm{u}) + \mathrm{N}^2 : 2\gamma^{\mathrm{nl}}(\mathrm{u}, \delta\mathrm{u})\big\} \mathrm{d}\Omega \tag{12c}$$

$$\big\langle \mathrm{M}(\mathrm{U}), \delta\mathrm{U}\big\rangle = \rho\mathrm{h} \int_\Omega \{\mathrm{u}\delta\mathrm{u} + \mathrm{v}\delta\mathrm{v} + \mathrm{w}\delta\mathrm{w}\} \mathrm{d}\Omega \tag{12d}$$

Herein, one searches the nonlinear fundamental frequency and its associated mode shape in the pre- or post-buckling ranges of the plate. Hence, the following coupled problems must to be solved:

$$\overline{\mathrm{L}}\big(\mathrm{U}^{\mathrm{s}}\big) + \overline{\mathrm{Q}}\big(\mathrm{U}^{\mathrm{s}}, \mathrm{U}^{\mathrm{s}}\big) - \lambda F = 0 \tag{13a}$$

$$\mathrm{L}(\mathrm{U}) + 2\mathrm{Q}\big(\mathrm{U}^{\mathrm{s}}, \mathrm{U}\big) + \mathrm{Q}(\mathrm{U}, \mathrm{U}) - \omega^2 \mathrm{M}(\mathrm{U}) = 0 \tag{13b}$$

## 3. Solution by an asymptotic numerical method

In this section, we propose, first, to solve the static equilibrium problem (13a) by an asymptotic numerical method such as it was done in previous works and tested for various shells structures by Potier-Ferry and co-workers. The fundamental branch, the bifurcation point and the bifurcated branch are computed. Secondly, one searches the solution of the dynamic problem described by Eq. (13b) using ANM in the same manner as in the static one. The solution branches (static or dynamic) are obtained analytically in the vicinity of a starting point. To get the whole of the responses, Padé approximants and a continuation technique are adopted [18,19].

### *3.1. Static equilibrium*

#### *3.1.1. Computation of the solution branches*

The basic idea of the ANM consists in searching the solution branches of the nonlinear problem (13a) under an asymptotic expansion form in terms of a control parameter $a$. This expansion is investigated starting from a known and regular solution $(\mathrm{U}_0^{\mathrm{s}}, \lambda_0)$:

$$\mathrm{U}^{\mathrm{s}} - \mathrm{U}_0^{\mathrm{s}} = \sum_{r=1}^{n} a^r \mathrm{U}_r^{\mathrm{s}}, \qquad \lambda - \lambda_0 = \sum_{r=1}^{n} a^r \lambda_r \tag{14}$$

where $n$ is a truncation order and $a$ is defined by:

$$a = \big\langle \mathrm{u}^{\mathrm{s}} - u_0^{\mathrm{s}}, \mathrm{u}_1^{\mathrm{s}}\big\rangle + (\lambda - \lambda_0)\lambda_1 \tag{15}$$

By substituting Eq. (14) into Eq. (13a) and Eq. (15), respectively, and equating coefficients of like powers of $a$, one transforms the nonlinear problem into a sequence of linear ones solved by the finite-element method. For a large discussion of the supplementary condition (Eq. (15)), the reader will refer to [20].

#### *3.1.2. Detection of bifurcation points*

A bifurcation indicator well adapted to the ANM framework can be defined by introducing a fictitious perturbing force $\Delta\mu f$ in the plate for a given equilibrium deformed state $(\mathrm{U}^{\mathrm{s}}, \lambda)$. $\Delta\mu$ is the intensity of this force and $\Delta\mathrm{U}$ its associated response. By superposing the fictitious perturbation and the applied load and neglecting the second order terms, one gets the following auxiliary problem:

$$\mathrm{L_t}(\Delta\mathrm{U}) = \Delta\mu f \tag{16}$$

where $\mathrm{L_t}$ is the tangent operator at the equilibrium point $(\mathrm{U}^{\mathrm{s}}, \lambda)$. Eq. (16) constitutes a linear system with respect to $\Delta\mathrm{U}$ and $\Delta\mu$. To ensure the uniqueness of the solution of Eq. (16), an additional condition is introduced [21]. The problem is solved by ANM in the same manner as for the equilibrium path. The obtained approximation of $\Delta\mu(a)$ is highly accurate inside the validity range $[0, a_{max}]$. The bifurcation and the limit points correspond exactly to the values of the load for which the operator $L_t$ is singular, i.e. the roots of the indicator $\Delta\mu$.

$$\Delta\mu(a) = 0 \tag{17}$$

Note that recently Cochelin and Medale [22] have proposed a new bifurcation indicator based only on the behavior of the branching path.

*3.1.3. Computation of the post-buckling branch by the ANM*

The bifurcated branch is searched using an asymptotic expansion starting from the bifurcation point. Because of the tangent stiffness matrix is singular, the first step of the bifurcated branch is computed in a specific way. First, the tangent directions from the simple bifurcation point are obtained by the classical bifurcation analysis, which leads to the well-known quadratic bifurcation equation. Secondly, the linear problems resulting from the asymptotic expansion are solved via an extended system [21]. The next steps of the bifurcating branch are determined by the classical ANM.

*3.2. Nonlinear free vibrations of buckled plate*

The purpose of this subsection consists in solving the nonlinear free vibrations problem given by Eq. (13b) using the asymptotic numerical method. The fundamental frequency parameter $\omega$ and the associated mode shape U corresponding to nonlinear free vibrations of the plate about any equilibrium position of the pre- or post-buckled domain are determined using the following asymptotic expansion:

$$\mathrm{U} - \mathrm{U}_0 = \sum_{r=1}^{p} a^r \mathrm{U}_r, \qquad \omega^2 - \omega_0^2 = \sum_{r=1}^{p} a^r \omega_r \tag{18}$$

The control parameter of series Eq. (18) can be identified as the projection of the displacement increment $(\mathrm{U} - \mathrm{U}_0)$ and the frequency one $(\omega^2 - \omega_0^2)$ on the tangent vector $(\mathrm{U}_1, \omega_1)$.

$$a = \langle \mathrm{u} - \mathrm{u}_0, \mathrm{u}_1 \rangle + \big(\omega^2 - \omega_0^2\big)\omega_1 \tag{19}$$

By substituting Eq. (18) into Eq. (13b) and Eq. (19), and equating coefficients of like powers of $a$, one gets the following set of linear problems:
order 0

$$\mathrm{L}(\mathrm{U}_0) + 2\mathrm{Q}\big(\mathrm{U}^s, \mathrm{U}_0\big) + \mathrm{Q}(\mathrm{U}_0, \mathrm{U}_0) - \omega_0^2 \mathrm{M}(\mathrm{U}_0) = 0 \tag{20a}$$

order 1

$$\begin{aligned} &\mathrm{L}_t^0(\mathrm{U}_1) - \omega_0^2 \mathrm{M}(\mathrm{U}_1) = \omega_1 \mathrm{M}(\mathrm{U}_0) \\ &\langle \mathrm{u}_1, \mathrm{u}_1 \rangle + \omega_1 \omega_1 = 1 \\ &\vdots \end{aligned} \tag{20b}$$

order $p$ $(p > 1)$

$$\begin{aligned} &\mathrm{L}_t^0(\mathrm{U}_p) - \omega_0^2 \mathrm{M}(\mathrm{U}_p) = \omega_p \mathrm{M}(\mathrm{U}_0) + \sum_{r=1}^{p-1} \omega_r \mathrm{M}(\mathrm{U}_{p-r}) - \sum_{r=1}^{p-1} \mathrm{Q}(\mathrm{U}_r, \mathrm{U}_{p-r}) \\ &\langle \mathrm{u}_p, \mathrm{u}_1 \rangle + \omega_p \omega_1 = 0 \end{aligned} \tag{20c}$$

where $\mathrm{L}_t^0(\bullet) = \mathrm{L}(\bullet) + 2\mathrm{Q}(\mathrm{U}^s, \bullet) + 2\mathrm{Q}(\mathrm{U}_0, \bullet)$.

Note that $\omega_0$ is obtained with the procedure described by [13], its corresponding form $\mathrm{U}_0$, given by Eq. (20a), is deduced by the Newton–Raphson iterative algorithm. The problem is then analytically solved. In order to use a classical displacement finite element, it is convenient to return to a pure displacement formulation [14]. The expansion of the constitutive law gives:
order 0:

$$\mathrm{N}_0^1 = [\mathrm{C_m}] : \big\{2\gamma^{nl}\big(\mathrm{u}^s, \mathrm{u}_0\big)\big\}; \qquad \mathrm{N}_0^2 = [\mathrm{C_m}] : \big\{\gamma^{l}(\mathrm{u}_0) + \gamma^{nl}(\mathrm{u}_0, \mathrm{u}_0)\big\} \tag{21a}$$

order 1:

$$\mathrm{N}_1^1 = [\mathrm{C_m}] : \big\{2\gamma^{nl}\big(\mathrm{u}^s, \mathrm{u}_1\big)\big\}; \qquad \mathrm{N}_1^2 = [\mathrm{C_m}] : \big\{\gamma^{l}(\mathrm{u}_1) + 2\gamma^{nl}(\mathrm{u}_0, \mathrm{u}_1)\big\} \tag{21b}$$

order $p$ $(p > 1)$:

$$\mathrm{N}_p^1 = [\mathrm{C_m}] : \left\{2\gamma^{\mathrm{nl}}\left(\mathrm{u^s}, \mathrm{u}_p\right)\right\}; \qquad \mathrm{N}_p^2 = [\mathrm{C_m}] : \left\{\gamma^{\mathrm{l}}(\mathrm{u}_p) + 2\gamma^{\mathrm{nl}}(\mathrm{u}_0, \mathrm{u}_p) + \sum_{r=1}^{p-1} \gamma^{\mathrm{nl}}(\mathrm{u}_r, \mathrm{u}_{p-r})\right\} \tag{21c}$$

The insertion of Eqs. (21) into Eqs. (20) leads to a sequence of linear problems in pure displacement:
order 0:

$$\int_\Omega \Big\{2\gamma^{\mathrm{nl}}\left(\mathrm{u^s}, \delta\mathrm{u}\right) : [\mathrm{C_m}] : 2\gamma^{\mathrm{nl}}\left(\mathrm{u^s}, \mathrm{u}_0\right) + \frac{3}{4}\left(\gamma^{\mathrm{l}}(\delta\mathrm{u}) + 2\gamma^{\mathrm{nl}}(\mathrm{u}_0, \delta\mathrm{u})\right) : [\mathrm{C_m}] : \left(\gamma^{\mathrm{l}}(\mathrm{u}_0) + 2\gamma^{\mathrm{nl}}(\mathrm{u}_0, \mathrm{u}_0)\right) + \delta\kappa : [\mathrm{C_b}] : \kappa_0$$
$$+ \mathrm{N^s} : 2\gamma^{\mathrm{nl}}(\mathrm{u}_0, \delta\mathrm{u})\Big\}\mathrm{d}\Omega - \omega_0^2\rho \mathrm{h} \int_\Omega \{\mathrm{u}_0\delta\mathrm{u} + \mathrm{v}_0\delta\mathrm{v} + \mathrm{w}_0\delta\mathrm{w}\}\mathrm{d}\Omega = 0 \tag{22a}$$

Order 1:

$$\int_\Omega \Big\{2\gamma^{\mathrm{nl}}\left(\mathrm{u^s}, \delta\mathrm{u}\right) : [\mathrm{C_m}] : 2\gamma^{\mathrm{nl}}\left(\mathrm{u^s}, \mathrm{u}_1\right) + \frac{3}{4}\left(\gamma^{\mathrm{l}}(\delta\mathrm{u}) + 2\gamma^{\mathrm{nl}}(\mathrm{u}_0, \delta\mathrm{u})\right) : [\mathrm{C_m}] : \left(\gamma^{\mathrm{l}}(\mathrm{u}_1) + 2\gamma^{\mathrm{nl}}(\mathrm{u}_0, \mathrm{u}_1)\right) + \delta\kappa : [\mathrm{C_b}] : \kappa_1$$
$$+ \left(\frac{3}{4}\mathrm{N}_0^2 + \mathrm{N^s}\right) : 2\gamma^{\mathrm{nl}}(\mathrm{u}_1, \delta\mathrm{u})\Big\}\mathrm{d}\Omega - \omega_0^2\rho h \int_\Omega \{\mathrm{u}_1\delta\mathrm{u} + \mathrm{v}_1\delta\mathrm{v} + \mathrm{w}_1\delta\mathrm{w}\}\mathrm{d}\Omega$$
$$= \omega_1\rho h \int_\Omega \{\mathrm{u}_0\delta\mathrm{u} + \mathrm{v}_0\delta\mathrm{v} + \mathrm{w}_0\delta\mathrm{w}\}\mathrm{d}\Omega \tag{22b}$$

Order $p$ $(p > 1)$:

$$\int_\Omega \Big\{2\gamma^{\mathrm{nl}}\left(\mathrm{u^s}, \delta\mathrm{u}\right) : [\mathrm{C_m}] : 2\gamma^{\mathrm{nl}}\left(\mathrm{u^s}, \mathrm{u}_p\right) + \frac{3}{4}\left(\gamma^{\mathrm{l}}(\delta\mathrm{u}) + 2\gamma^{\mathrm{nl}}(\mathrm{u}_0, \delta\mathrm{u})\right) : [\mathrm{C_m}] : \left(\gamma^{\mathrm{l}}(\mathrm{u}_p) + 2\gamma^{\mathrm{nl}}(\mathrm{u}_0, \mathrm{u}_p)\right)$$
$$+ \delta\kappa : [\mathrm{C_b}] : \kappa_p + \left(\frac{3}{4}\mathrm{N}_0^2 + \mathrm{N^s}\right) : 2\gamma^{\mathrm{nl}}(\mathrm{u}_p, \delta\mathrm{u})\Big\}\mathrm{d}\Omega - \omega_0^2\rho h \int_\Omega \{\mathrm{u}_p\delta\mathrm{u} + \mathrm{v}_p\delta\mathrm{v} + \mathrm{w}_p\delta\mathrm{w}\}\mathrm{d}\Omega$$
$$= \omega_p\rho h \int_\Omega \{\mathrm{u}_0\delta\mathrm{u} + \mathrm{v}_0\delta\mathrm{v} + \mathrm{w}_0\delta\mathrm{w}\}\mathrm{d}\Omega + \sum_{r=1}^{p-1} \omega_p\rho h \int_\Omega \{\mathrm{u}_{p-r}\delta\mathrm{u} + \mathrm{v}_{p-r}\delta\mathrm{v} + \mathrm{w}_{p-r}\delta\mathrm{w}\}\mathrm{d}\Omega$$
$$- \frac{3}{4}\sum_{r=1}^{p-1}\int_\Omega \left\{\mathrm{N}_r^2 : 2\gamma^{\mathrm{nl}}(\mathrm{u}_{p-r}, \delta\mathrm{u}) + \left(\gamma^{\mathrm{l}}(\delta\mathrm{u}) + 2\gamma^{\mathrm{nl}}(\mathrm{u}_0, \delta\mathrm{u})\right) : [\mathrm{C_m}] : \gamma^{\mathrm{nl}}(\mathrm{u}_r, \mathrm{u}_{p-r})\right\}\mathrm{d}\Omega \tag{22c}$$

### *3.3. Discretization by the finite element method*

For the static equilibrium branches and the bifurcation indicator, details about the finite element discretization used in this paper are given in [21]. For the nonlinear vibrations problem, the discretization of Eq. (22a) and its solution by a classical Newton–Raphson procedure permits to get the starting point $(\mathrm{U}_0, \omega_0)$. The discretized forms of Eq. (22b) and Eq. (22c) get:
order 1:

$$\begin{aligned} &\left[\mathrm{K_t^0} - \omega_0^2\mathrm{M}\right]\{\mathrm{q}_1\} = \omega_1\mathrm{M}\{\mathrm{q}_0\} \\ &\langle \mathrm{q}_1, \mathrm{q}_1\rangle + \omega_1\omega_1 = 1 \end{aligned} \tag{23}$$

order $p$ $(p > 1)$:

$$\begin{aligned} &\left[\mathrm{K_t^0} - \omega_0^2\mathrm{M}\right]\{\mathrm{q}_p\} = \omega_p\mathrm{M}\{\mathrm{q}_0\} + \left\{\mathrm{F}_p^{\mathrm{nl}}\right\} \\ &\langle \mathrm{q}_1, \mathrm{q}_p\rangle + \omega_1\omega_p = 0 \end{aligned} \tag{24}$$

where $\mathrm{K_t^0}$ corresponds to the elastic stiffness matrix and M to the mass one, $\{\mathrm{q}_p\}$ is the modal displacement vector of order $p$ and the vectors $\{\mathrm{F}_p^{\mathrm{nl}}\}$ is obtained from the right-hand side of Eq. (22c). Indeed, the series of Eq. (18) have a radius of convergence limiting its validity range, but this can be largely improved using Padé approximants [18,19]:

$$U - U_0 = \sum_{i=1}^{n-1} f_i(a) a^i U_i,$$
$$\omega^2 - \omega_0^2 = \sum_{i=1}^{n-1} f_i(a) a^i \omega_i \tag{25}$$

where $f_i(a)$ are rational fractions having the same denominator and the vectors $U_i$ are obtained from U by the classical Gram–Schmidt orthogonalization procedure. The validity range of the solution Eq. (25) is defined by the maximal value $a_{max}$ of the control parameter $a$ requiring that the relative difference between the displacements at two consecutive orders must be smaller than a given parameter $\delta$:

$$\delta = \frac{\| u_n^p(a_{max}) - u_{n-1}^p(a_{max}) \|}{\| u_n^p(a_{max}) - u_0^p \|} \tag{26}$$

The principal steps of the proposed algorithm are organized as follows:

**Computation of equilibrium branches**

Step 1: Computation of a solution path

Evaluation of the solution at order 1:

Solve: $[K_t^0]\{\overline{U}_1^L\} = \{F\}$

Compute: $\lambda_1 = 1/\sqrt{1 + \langle \overline{U}_1^L, \overline{U}_1^L \rangle}$, $\{U_1^s\} = \lambda_1 \{\overline{U}_1^L\}$

Compute: $N_1^s = [C_m] : \{\gamma^L(U_1^s) + 2\gamma^{NL}(U_0^s, U_1^s)\}$

Evaluation of the solution at order $p$:

Solve: $[K_t^0]\{\overline{U}_p^{NL}\} = \{\overline{F}_p^{NL}\}$

Compute: $\lambda_p = -\lambda_1 \langle \overline{U}_p^{NL}, U_1^s \rangle$, $\{U_p^s\} = \frac{\lambda_p}{\lambda_1}\{U_1^s\} + \{\overline{U}_p^{NL}\}$

Compute: $N_p^s = [C_m] : \{\gamma^L(U_p^s) + 2\gamma^{NL}(U_0^s, U_p^s) + \sum_{r=1}^{p-1} \gamma^{NL}(U_r^s, U_{p-r}^s)\}$

Step 2: Detection of bifurcation points

Evaluation of the solution at order 0:

Solve: $[K_t^0]\{\Delta U_0\} = \Delta\mu_0 \{f\}$ with $\Delta\mu_0 = 1$

Evaluation of the solution at order $p \geq 1$:

Solve: $[K_t^0]\{\Delta \overline{U}_p\} = \{\Delta F_p\}$

Compute: $\Delta\mu_p = -\frac{\langle \Delta F_p, \Delta U_0 \rangle}{\langle f, \Delta U_0 \rangle}$, $\{\Delta U_p\} = \Delta\mu_p \{\Delta U_0\} + \{\Delta \overline{U}_p\}$

[3pt] Compute: $\Delta N_p = [C_m] : \{\gamma^L(\Delta U_p) + 2\gamma^{NL}(U_0^s, \Delta U_p) + \sum_{r=1}^{p} 2\gamma^{NL}(U_r^s, \Delta U_{p-r})\}$

If $\Delta\mu = 0$, compute $(U_c, \lambda_c, \phi)$, go to step 3

Else return to step 1

Step 3: Computation of a bifurcating branch

Evaluation of the solution at order 1:

Solve: $[K_t^c]\{W\} = \{F\}$

Compute: $d = \langle \phi, \overline{Q}(W, W) \rangle$ $b = \langle \phi, \overline{Q}(\phi, \phi) \rangle$ $c = \langle \phi, \overline{Q}(W, \phi) \rangle$

Compute: $\eta_1 = 1/\sqrt{\langle \phi, \phi \rangle + (1 + \langle W, W \rangle)(\frac{-c \pm \sqrt{c^2 - db}}{d})^2}$, $\lambda_1 = \eta_1 \frac{-c \pm \sqrt{c^2 - db}}{d}$

Compute: $U_1 = \lambda_1 W + \eta_1 \phi$

Evaluation of the solution at order $p$:

Solve: $[K_t^c]\{\hat{U}_p\} = \{F_p\}$

Compute: $\hat{N}_p = [C_m] : \{\gamma^L(\hat{U}_p) + 2\gamma^{NL}(U_c, \hat{U}_p) + \sum_{r=1}^{p-1} \gamma^{NL}(U_r^s, U_{p-r}^s)\}$

Compute: $\beta = \langle \phi, Q(U_1^s, \hat{U}_p) \rangle + \frac{1}{2} \sum_{r=1}^{p-1} \langle \phi, Q(U_r^s, U_{p+1-r}^s) \rangle$

Solve: $\begin{bmatrix} \lambda_1 d + \eta_p c & \lambda_1 c + \eta_p b \\ \lambda_1 + \langle W, U_1^s \rangle & \langle \phi, U_1^s \rangle \end{bmatrix} \begin{Bmatrix} \lambda_p \\ \eta_p \end{Bmatrix} = -\begin{bmatrix} \beta \\ \langle \hat{U}_p, U_1^s \rangle \end{bmatrix}$

Compute: $U_p = \lambda_p W + \eta_p \phi + \hat{U}_p$

**Nonlinear vibration of buckled plate for any static equilibrium**

Solution of the problem at order 0:

Solve: $[\mathrm{K_e} - \omega_0^2 \mathrm{M}]\{\mathrm{U}_0\} = 0$

Compute: $\mathrm{N}_0^1 = [\mathrm{C_m}] : \{2\gamma^{\mathrm{nl}}(\mathrm{U^s}, \mathrm{U}_0)\}$, $\mathrm{N}_0^2 = [\mathrm{C_m}] : \{\gamma^{\mathrm{l}}(\mathrm{U}_0) + \gamma^{\mathrm{nl}}(\mathrm{U}_0, \mathrm{U}_0)\}$

Solution of the problem at order 1:

Solve: $[\mathrm{K_t^0} - \omega_0^2 \mathrm{M}]\{\hat{\mathrm{U}}_1\} = \mathrm{M}\{\mathrm{U}_0\}$

Compute $\omega_1 = 1/\sqrt{1 + \langle \hat{\mathrm{U}}_1,\ \hat{\mathrm{U}}_1 \rangle}$, $\{\mathrm{U}_1\} = \omega_1 \{\hat{\mathrm{U}}_1\}$

Compute $\mathrm{N}_1^1 = [\mathrm{C_m}] : \{2\gamma^{\mathrm{nl}}(\mathrm{U^s}, \mathrm{U}_1)\}$, $\mathrm{N}_1^2 = [\mathrm{C_m}] : \{\gamma^{\mathrm{l}}(\mathrm{U}_1) + 2\gamma^{\mathrm{nl}}(\mathrm{U}_0, \mathrm{U}_1)\}$

Solution of the problem at order $p$:

Solve: $[\mathrm{K_t^0} - \omega_0^2 \mathrm{M}]\{\hat{\mathrm{U}}_p\} = \{\mathrm{F}_p^{\mathrm{nl}}\}$

Compute: $\omega_p = -\omega_1 \langle \hat{\mathrm{U}}_p, \mathrm{U}_1 \rangle$, $\{\mathrm{U}_p\} = \frac{\omega_p}{\omega_1}\{\mathrm{U}_1\} + \{\hat{\mathrm{U}}_p\}$

Compute: $\mathrm{N}_p^1 = [\mathrm{C_m}] : \{2\gamma^{\mathrm{nl}}(\mathrm{U^s}, \mathrm{U}_p)\}$,

$\mathrm{N}_p^2 = [\mathrm{C_m}] : \{\gamma^{\mathrm{l}}(\mathrm{U}_p) + 2\gamma^{\mathrm{nl}}(\mathrm{U}_0, \mathrm{U}_p) + \sum_{r=1}^{p-1} \gamma^{\mathrm{nl}}(\mathrm{U}_r, \mathrm{U}_{p-r})\}$

## 4. Numerical results

To show the efficiency and the applicability of the proposed algorithm, one considers the nonlinear free vibration of pre or post buckled isotropic homogeneous rectangular plate of length $L$, width $l$ and thickness $h = 1$ mm. The used material properties are: Young's modulus $E = 70$ GPa, Poisson's ratio $\nu = 0.3$ and mass density $\rho = 2778$ kg/m$^3$. For the discretization of the plate, a DKT triangular shell element having three nodes and six degrees of freedom per node $(u, v, w, \theta_x, \theta_y, \theta_z)$ is adopted [23,24]. For symmetry reasons, only a quarter of the plate is modeled. In the present study, four boundary conditions are considered: simply supported with movable edges $\{(w = \theta_x = 0$ at $x = 0$ and $x = L)$ and $(w = \theta_y = 0$ at $y = 0$ and $y = l)\}$, simply supported with immovable edges $\{(u = v = w = \theta_x = 0$ at $x = 0$ and $x = L)$ and $(u = v = w = \theta_y = 0$ at $y = 0$ and $y = l)\}$, clamped with movable edges $(w = \theta_x = \theta_y = 0$ at all edges) and clamped with immovable edges $(u = v = w = \theta_x = \theta_y = 0$ at all edges). The adopted parameters are nondimensionalized as follows: the nonlinear frequency is nondimensionalized with respect to its corresponding linear frequency $\omega^* = \omega/\omega_0$, the axial load with respect to its corresponding critical buckling load, $\lambda^* = \lambda/\lambda_c$, and the maximum amplitude with respect to the thickness $W$ (center)/$h$. As it was shown in previous works [13,25], one takes a truncation order $n = 20$ and an accuracy parameter $\delta = 10^{-4}$. To improve the validity range of the series and to reduce the computational cost, Padé approximants are incorporated at each stage of the procedure. In Fig. 2a and b, one presents, respectively, the static equilibrium branches of clamped and simply supported plates with movables edges and subjected to uniaxial compression for various aspect ratios. These responses are determined using the procedure described in Subsection 3.1 and largely discussed in previous works [13]. They present a fundamental branch (pre-buckling), a bifurcation point and a bifurcated branch (post buckling). The fictitious perturbation force associated with the bifurcation indicator is concentrated and normal to the middle surface of the plate. The fundamental branch is obtained by only one step and the bifurcated one by only two steps for the two examples. As is well known, these bifurcations are symmetric and stable. Beyond the bifurcation points, the fundamental branch becomes instable and the bifurcated one is stable. It is then important to study the oscillations of the structure around these equilibrium states.

In order to verify the validity and the accuracy of the proposed methodology (formulation and computer program), one considers the nonlinear free vibrations of unloaded clamped and simply supported plates with immovable edges. In Table 1, one compares the results obtained by the present method and those reported by Azrar using an asymptotic numerical method [16] or a finite element method [26]; a good agreement is observed between these approaches. In Fig. 3, one illustrates the backbone curves of the nonlinear fundamental frequency $\omega^* = \omega/\omega_L$ for a clamped and simply supported plates with movable edges. These nonlinearities are of hard types.

In Fig. 4, one presents backbone curves of the fundamental frequency of nonlinear vibrations of a clamped plate with movable edges about a static equilibrium of the pre buckled domain for various aspect ratios $(L/l)$. One notes that the linear fundamental frequency $\omega_0$ is first determined by the procedure described in [13]. The starting vector $\mathrm{U}_0$, used in Eq. (18), is secondly deduced using the Newton–Raphson algorithm. One observes that an increase in the applied load induces a shift of backbone curves to the left. In Fig. 5, one gives backbone curves related to a nonlinear free vibration of the considered plate about a post buckled equilibrium state. Contrary to the previous case, an increase in the applied load induces a shift of the backbone curves to the right. In the transition domain from the pre-buckling equilibrium to the post-buckling one, the response seems to be linear for small amplitudes. Moreover, for aspect ratio values equal to 1.75 or 2 and when $\lambda^*$ is close to 1, instability phenomena are observed with loops or limit points (Figs. 4d and 5d) inducing generally a jumping

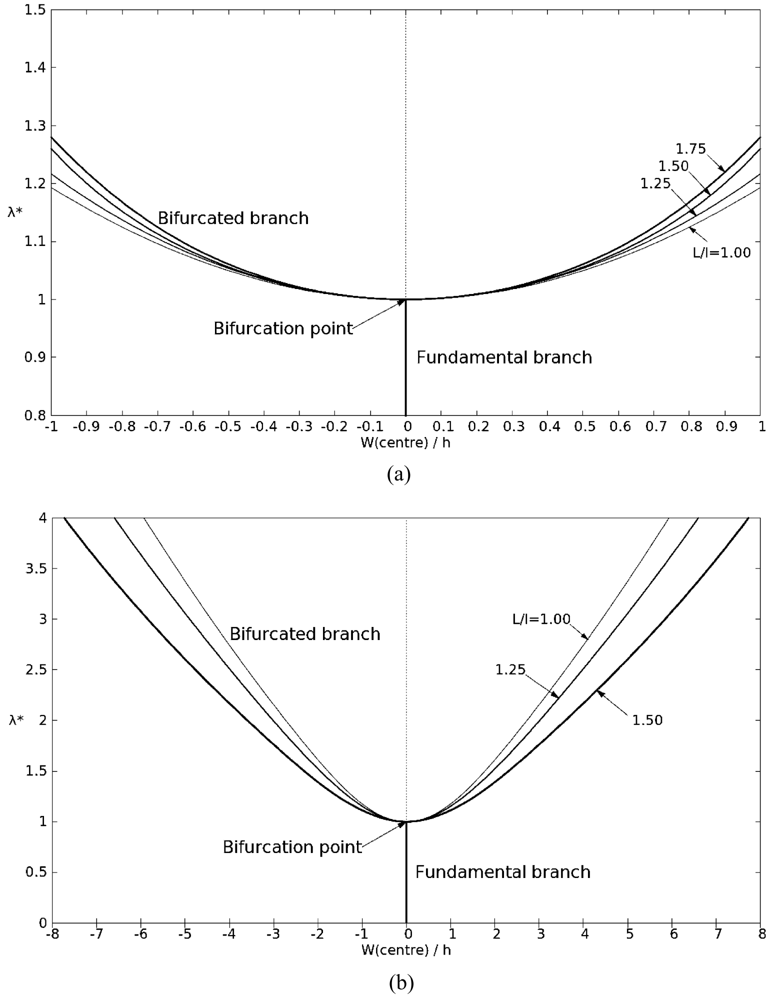


**Fig. 2.** Influence of the aspect ratio ($L/l$) on the static response of plates with movable edges subjected to uniaxial load: (a) clamped, (b) simply supported.

**Table 1**
Frequency ratio $\omega/\omega_L$ according to the maximum amplitude at the center $W$ (center)/$h$ of an isotropic square plate with various boundary conditions.

| Present results | | $W$ (center)/$h$ | $\omega/\omega_L$ | |
|---|---|---|---|---|
| $W$ (center)/$h$ | $\omega/\omega_L$ | | Results [Azrar] | Results [FEM] |
| Simply supported | | | | |
| 0.20000475 | 1.02026 | 0.2 | 1.01976 | 1.0196 |
| 0.40000744 | 1.07889 | 0.4 | 1.07669 | 1.0763 |
| 0.60001124 | 1.17103 | 0.6 | 1.16596 | 1.1645 |
| 0.80001297 | 1.28906 | 0.8 | 1.28124 | 1.2779 |
| 1.00000150 | 1.42851 | 1.0 | 1.41666 | 1.4109 |
| Clamped | | | | |
| 0.20003733 | 1.00744 | 0.2 | 1.00723 | 1.0073 |
| 0.40006206 | 1.02933 | 0.4 | 1.02860 | 1.0291 |
| 0.60008235 | 1.06459 | 0.6 | 1.06321 | 1.0648 |
| 0.80004972 | 1.11215 | 0.8 | 1.10975 | 1.1138 |
| 1.00009200 | 1.17135 | 1.0 | 1.16672 | 1.1762 |

of the structure between different equilibrium positions. But, in the case of a square plate, for instance, and following the tests carried out, these phenomena are not detected. In Figs. 6 and 7, one presents backbone curves corresponding to the nonlinear fundamental frequency of a simply supported plate with respect to the aspect ratio and applied load ratio in

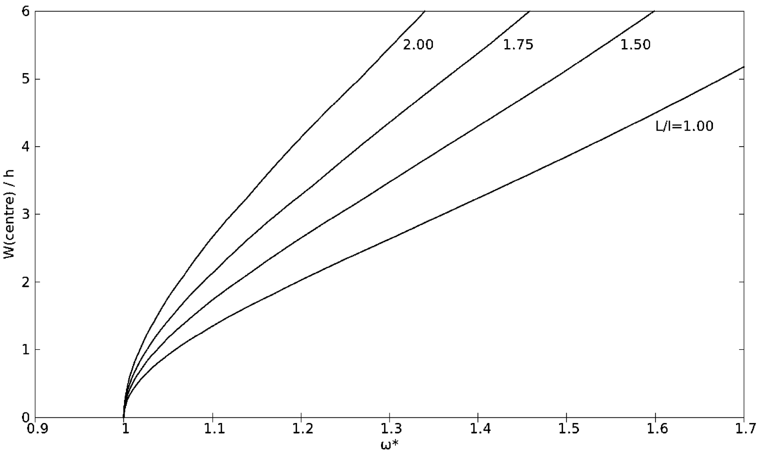


(a)

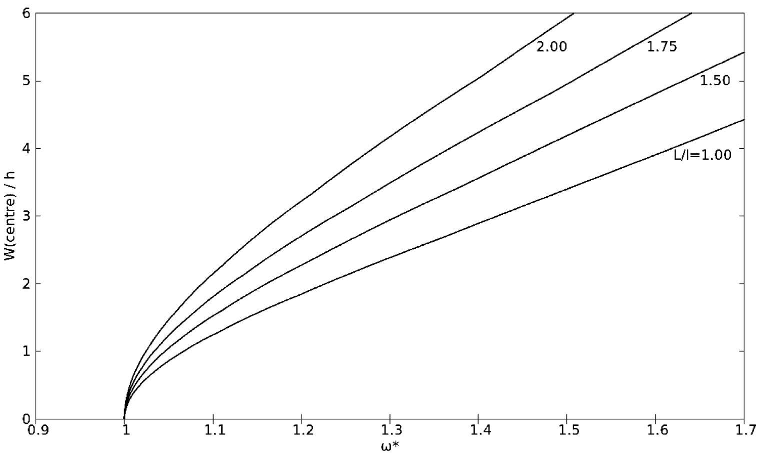


(b)

**Fig. 3.** Influence of the aspect ratio ($L/l$) of unloaded plates with immovable edges on the backbone curves of nonlinear vibration fundamental frequency: (a) clamped, (b) simply supported.

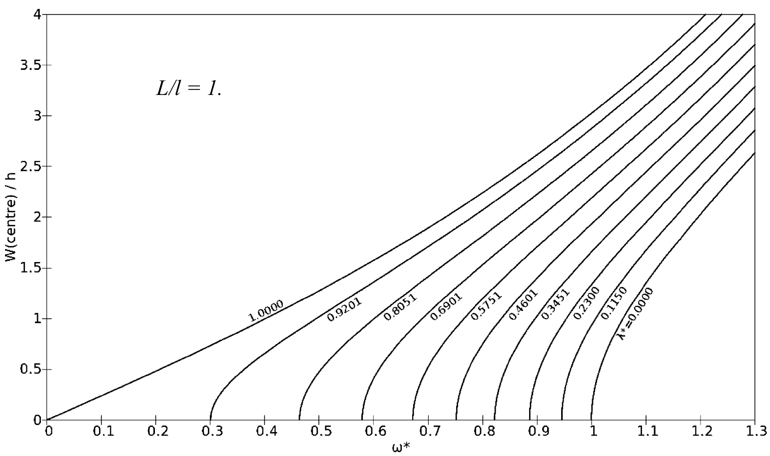


(a)

**Fig. 4.** Clamped plate with movable edges: Influence of the applied load ratio on the backbone curve of the fundamental frequency of nonlinear vibrations of the plate about a static equilibrium of the pre buckled domain for various aspect ratios $L/l$: a (1), b (1.5), c (1.75), d (2).

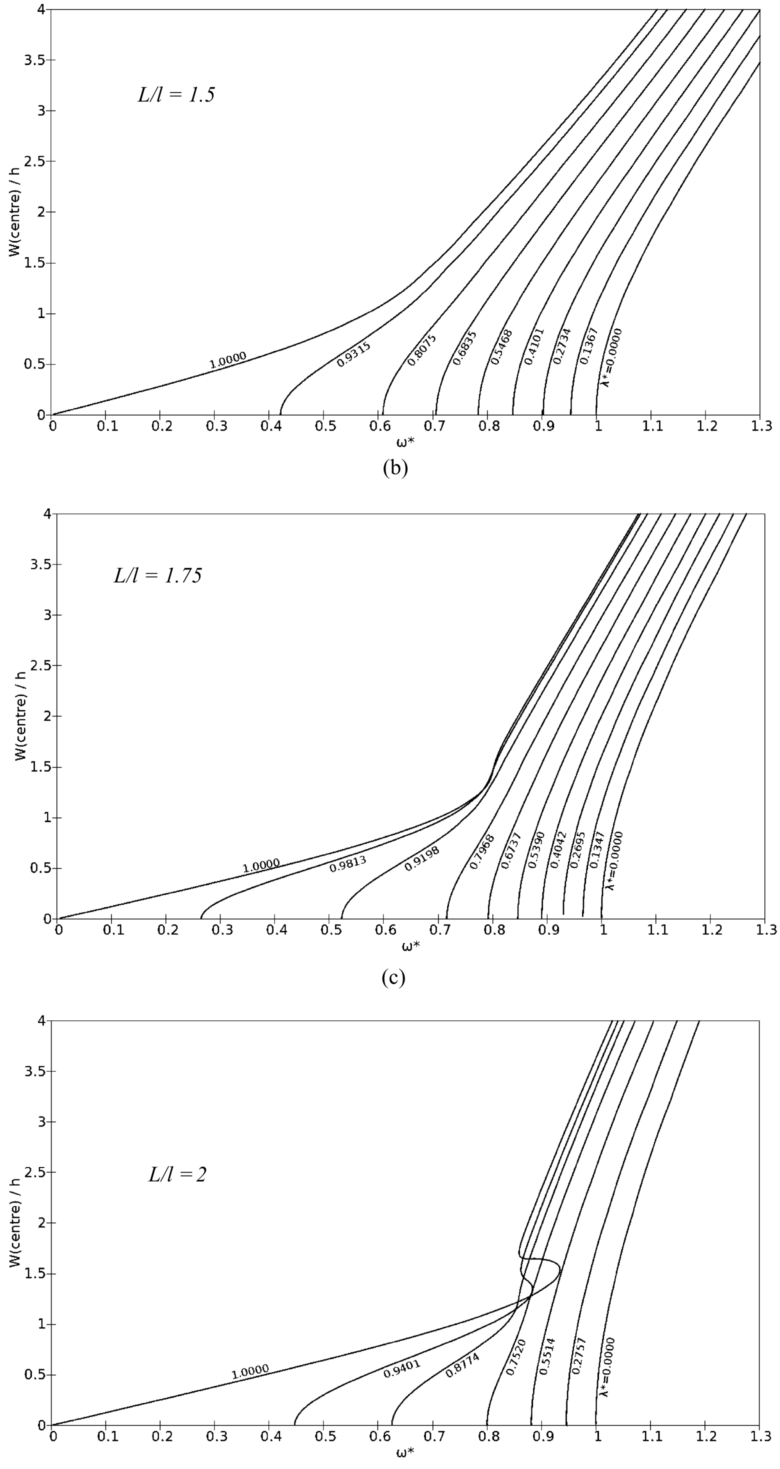


**Fig. 4.** (*continued*)

pre-buckled or post-buckled domain, respectively. Compared to the last tests, the same phenomena are practically observed. The major difference lies in the fact that, for a given nonlinear frequency, the displacement amplitudes are large for the clamped plate.

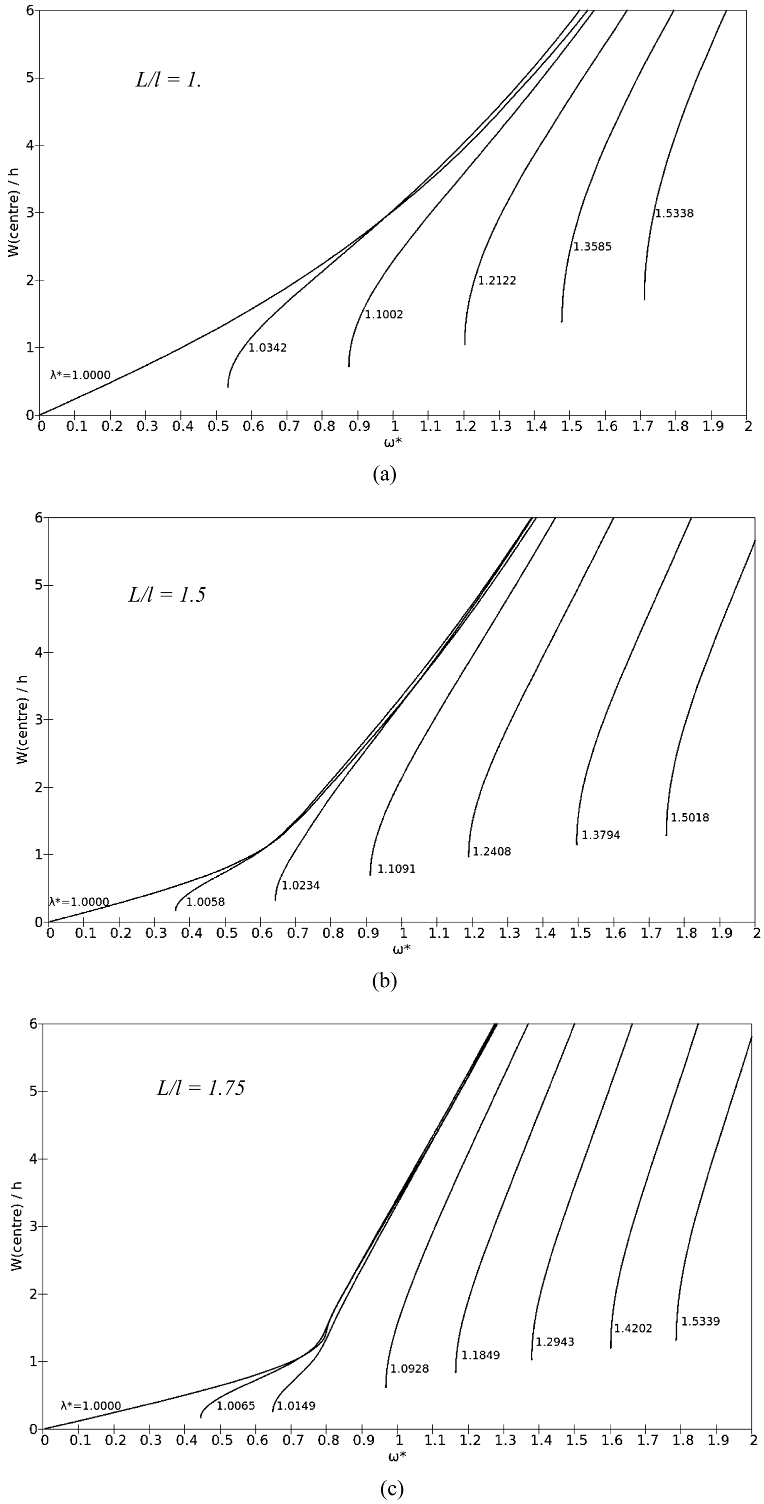


**Fig. 5.** Clamped plate with movable edges: influence of the applied load ratio on the backbone curve of the fundamental frequency of nonlinear vibrations of the plate about a static equilibrium of the post-buckled domain for various aspect ratios $L/l$: a (1), b (1.5), c (1.75), d (2).

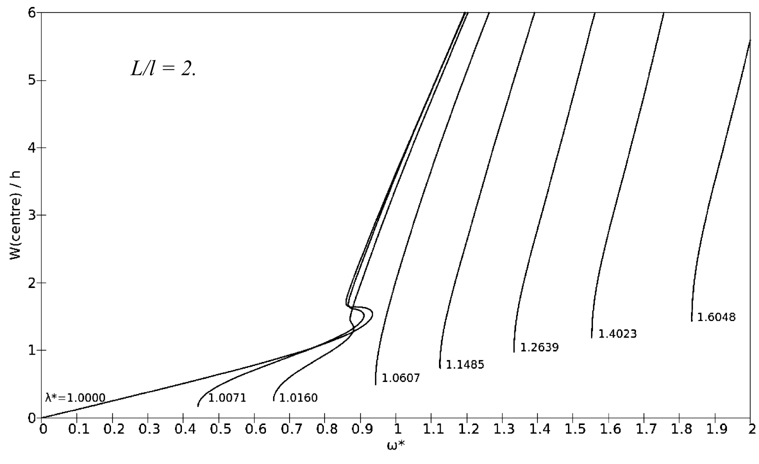


(d)

**Fig. 5.** (*continued*)

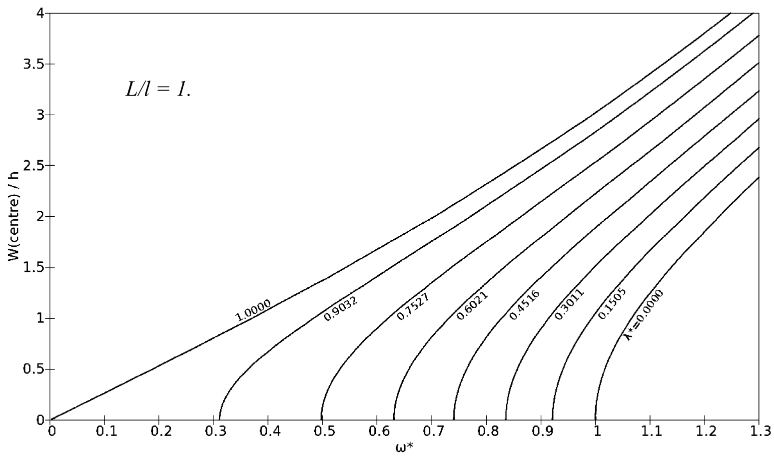


(a)

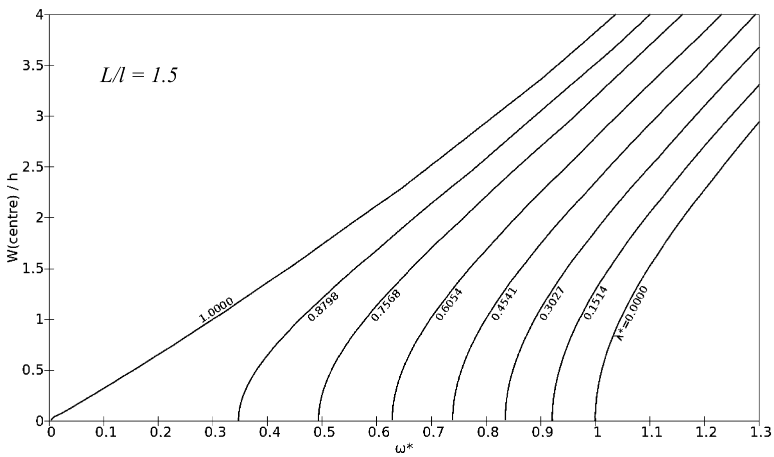


(b)

**Fig. 6.** Simply supported plate with movable edges: influence of the applied load ratio on the backbone curve of the fundamental frequency of nonlinear vibrations of the plate about a static equilibrium of the pre-buckled domain for various aspect ratios $L/l$: a (1), b (1.5), c (2).

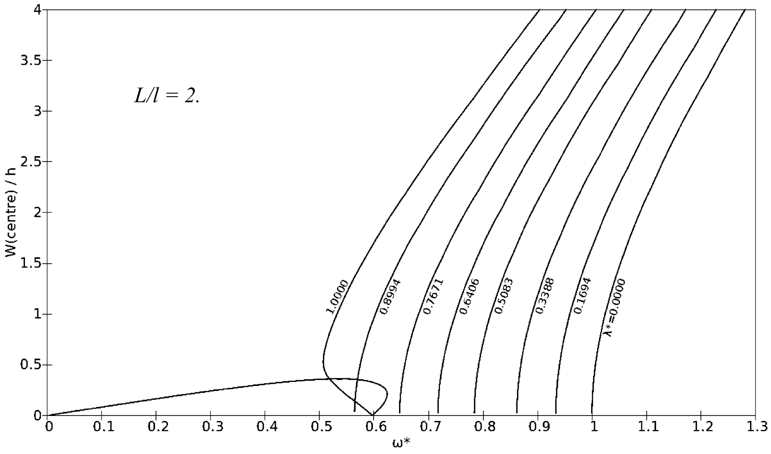


(c)

**Fig. 6.** (*continued*)

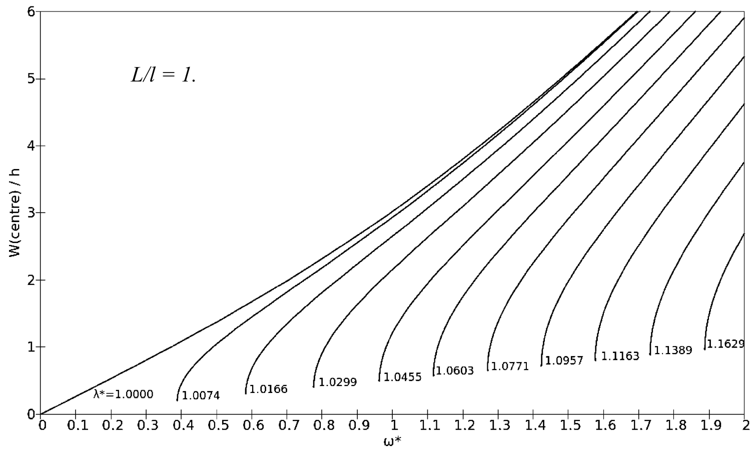


(a)

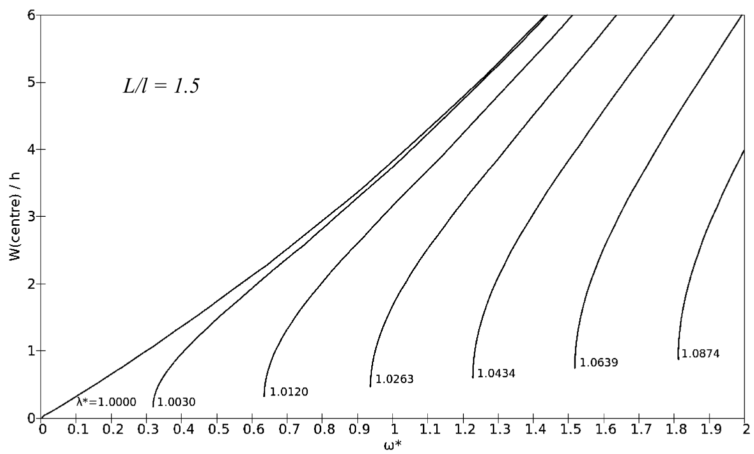


(b)

**Fig. 7.** Simply supported plate with movable edges: influence of the applied load ratio on the backbone curve of the fundamental frequency of nonlinear vibrations of the plate about a static equilibrium of the post buckled domain for various aspect ratios $L/l$: a (1), b (1.5), c (2).

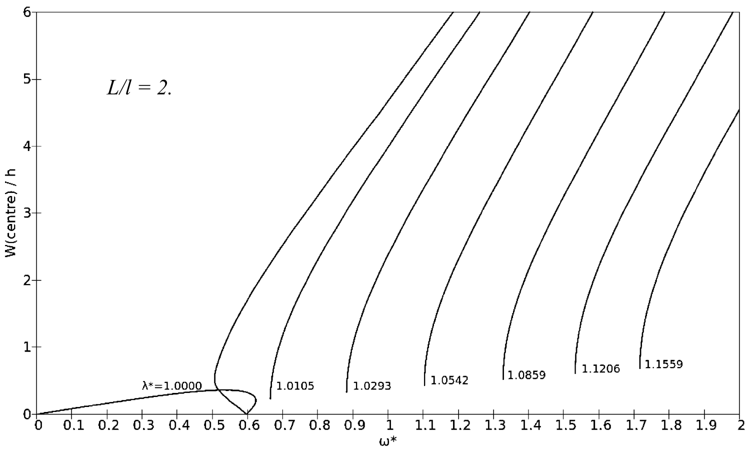


(c)

**Fig. 7.** (*continued*)

## 5. Conclusion

In this study, we have presented a methodological approach based on the asymptotic numerical method and harmonic balance method for the investigation of the nonlinear free vibrations of buckled von Karman plate. The coupled nonlinear problems (static and dynamic) are transformed into a sequence of linear ones with only two operators to be inverted. The backbone curves of the fundamental frequency of nonlinear vibrations of the plate, about any static equilibrium corresponding to pre- or post-buckled domain, are obtained automatically. The incorporation of Padé approximants at each stage of the algorithm permits a large reduction of the computational cost. The realized numerical tests show the effectiveness and the reliability of the proposed methodology. It will be interesting to extend the analysis to other structures subjected to various load types.

## References

[1] R.G. White, Effects of non-linearity due to large deflections in the resonance testing of structures, J. Sound Vib. 16 (1971) 255–267.
[2] J.B. Min, J.G. Eisley, Nonlinear vibration of buckled beams, J. Eng. Ind. (1972) 637–645.
[3] W.Y. Tseng, J. Dugundji, Nonlinear vibrations of a buckled beam under harmonic excitation, J. Appl. Mech. (1971) 467–476.
[4] W. Lestari, S. Hanagud, Nonlinear vibration of buckled beams: some exact solutions, Int. J. Solids Struct. 38 (2001) 4741–4757.
[5] M.H. Mahdavi, L.Y. Jiang, X. Sun, Nonlinear vibration and postbuckling analysis of a single layer graphene sheet embedded in a polymer matrix, Physica E 44 (2012) 1708–1715.
[6] M. Faghih Shojaei, R. Ansari, V. Mohammadi, H. Rouhi, Nonlinear forced vibration analysis of postbuckled beams, Arch. Appl. Mech. 84 (2014) 421–440.
[7] R. Ansari, M.A. Ashrafi, A. Arjangpay, An exact solution for vibrations of post-buckled microscale beams based on the modified couple stress theory, Appl. Math. Model. 39 (2015) 3050–3062.
[8] S. Sahmani, M. Bahrami, R. Ansari, Surface effects on the free vibration behavior of postbuckled circular higher-order shear deformable nanoplates including geometrical nonlinearity, Acta Astronaut. 105 (2014) 417–427.
[9] J. Girish, L.S. Ramachandra, Thermal postbuckled vibrations of symmetrically laminated composite plates withe initial geometric imperfections, J. Sound Vib. 282 (2005) 1137–1153.
[10] S.R. Li, Y.H. Zhou, X. Song, Non-linear vibration and thermal buckling of an orthotropic annular plate with a centric rigid mass, J. Sound Vib. 251 (2002) 141–152.
[11] X.K. Xia, H.S. Shen, Vibration of postbuckled FGM hybrid laminated plates in thermal environment, Eng. Struct. 30 (2008) 2420–2435.
[12] X.K. Xia, H.S. Shen, Vibration of post-buckled sandwich plates with FGM face sheets in a thermal environment, J. Sound Vib. 314 (2008) 254–274.
[13] E.H. Boutyour, L. Azrar, M. Potier-Ferry, Vibration of buckled elastic structures with large rotations by an asymptotic numerical method, Comput. Struct. 84 (2006) 93–101.
[14] B. Cochelin, A path following technique via an asymptotic numerical method, Comput. Struct. 53 (1994) 1181–1192.
[15] A.H. Nayfeh, D.T. Mook, Non-Linear Oscillations, Wiley, New York, USA, 1979.
[16] L. Azrar, R. Benamar, M. Potier-Ferry, An asymptotic–numerical method for large-amplitude free vibrations of thin elastic plates, J. Sound Vib. 220 (1999) 695–727.
[17] L. Azrar, E.H. Boutyour, M. Potier-Ferry, Non-linear forced vibrations of plates by an asymptotic–numerical method, J. Sound Vib. 252 (2002) 657–674.
[18] A. Elhage-Hussein, M. Potier-Ferry, N. Damil, A numerical continuation method based on Padé approximants, Int. J. Solids Struct. 37 (2000) 6981–7001.
[19] A. Najah, B. Cochelin, N. Damil, M. Potier Ferry, A critical review of asymptotic numerical methods, Arch. Comput. Methods Eng. 5 (1998) 3–22.
[20] H. Mottaqui, B. Braikat, N. Damil, Discussion about parameterization in the asymptotic numerical method: application to nonlinear elastic shells, Comput. Methods Appl. Mech. Eng. 199 (2010) 1701–1709.
[21] E.H. Boutyour, Méthode asymptotique–numérique pour le calcul des bifurcations : application aux structures élastiques, Thesis, Université de Metz, France, 1994.
[22] B. Cochelin, M. Medale, Power series analysis as a major breakthrough to improve the efficiency of asymptotic numerical method in the vicinity of bifurcations, J. Comput. Phys. 236 (2013) 594–607.
[23] O.C. Zienkiewicz, The Finite Element Method, 3rd edition, McGraw-Hill, London, UK, 1977.

[24] J.L. Batoz, G. Dhatt, Modélisation des structures par éléments finis, Hermès, Paris, France, 1990.
[25] E.H. Boutyour, H. Zahrouni, M. Potier-Ferry, M. Boudi, Bifurcation points and bifurcated branches by an asymptotic numerical method and Padé approximants, Int. J. Numer. Methods Eng. 60 (2004) 1987–2012.
[26] S.L. Lau, Y.K. Cheung, S.Y. Wu, Nonlinear vibration of thin elastic plates. Part I: Generalised incremental Hamilton's principle and finite element formulation, J. Appl. Mech. 51 (1984) 837–844.